Azomethines with Long Alkyl Chains: Synthesis, Characterization, Biological Properties and logP Modelling

Nikita Yurievich Serov *, Khasan Rafaelevich Khayarov, Irina Vasilevna Galkina, Marina Petrovna Shulaeva, Vyacheslav Alekseevich Grigorev, Timur Rustemovich Gimadiev

Posted Date: 23 December 2025

doi: 10.20944/preprints202512.1855.v1

Keywords: azomethines; antibacterial activity; lipophilicity; quantum chemistry; machine learning

 doi:10.20944/preprints202512.1855.v1

Article

Azomethines with Long Alkyl Chains: Synthesis, Characterization, Biological Properties and logP Modelling

Nikita Yu. Serov [1,2,*], Khasan R. Khayarov [2], Irina V. Galkina [2], Marina P. Shulaeva [3], Vyacheslav A. Grigorev [2] and Timur R. Gimadiev [1,2]

[1] Federal Research Center "Kazan Scientific Center of the Russian Academy of Sciences", Kazan, 420111, Russian Federation

[2] A.M. Butlerov Chemical Institute, Kazan Federal University, Kazan, 420008, Russian Federation

[3] Kazan State Medical Academy, Kazan, 420012, Russian Federation

* Correspondence: serov.nikita@gmail.com

Abstract

The search of new antibacterial agents is an important task due to the emergence of resistance to widely used drugs. The bromine, chlorine and nitro-substituted in phenyl ring azomethines with long alkyl chains (C12, C14, C16 and C18) were synthesized and characterized by several experimental methods (NMR and IR spectroscopy, elemental analysis). Antibacterial activity was tested on several cultures and the synthesized compounds show the activity at the level of some commercial antiseptics. Lipophilicity (which is important descriptor for biological properties prediction) of the experimentally synthesized and isomeric molecules was determined by three different approaches: quantum chemistry, machine learning (GraphormerLogP model) and atom contribution model (RDKit library). Quantum-chemical method can take into account any spatial arrangements and can be considered the most accurate of the used approaches, but a lot of computational time it is necessary for it. Atom contribution model is the fastest of the used methods but gives underestimated results and different isomers have exactly the same values in contrast to the quantum chemistry results. Machine learning-based methods (GraphormerLogP) demonstrate acceptable accuracy, sensitivity to isomerism, and orders of magnitude higher throughput, making them an optimal tool for high-throughput screening.

Keywords: azomethines; antibacterial activity; lipophilicity; quantum chemistry; machine learning

1. Introduction

One of the actual tasks of modern chemistry is the search of new pharmacologically active substances. This is due to the need to create drugs against new diseases, reduce toxicity and side effects, and improve the effectiveness of existing drugs. Additional problem, which leads to the need to search for new antibacterial agents, is the developing bacterial resistance to widely used substances. A known direction for the obtaining of new biologically active compounds is the functionalization of known biologically active molecules.

Azomethines, commonly known as Shiff bases, have firmly established their importance in modern chemical research due to their remarkable versatility and wide-ranging applications, particularly in the fields of medical chemistry [1–4] and advanced materials science. These compounds, characterized by the imine group >C=N-, serve as pivotal ligands in coordination chemistry, forming complexes with diverse metal ions that exhibit biological activity [5,6], magnetic behavior and photoluminescent properties.

Numerous studies have documented that azomethines exhibit significant antibacterial properties [7,8], demonstrating effectiveness against pathogens such as *Staphylococcus aureus* and

 doi:10.20944/preprints202512.1855.v1

Escherichia coli, with some compounds showing activity comparable to standard antibiotics like Ciprofloxacin [8]. Beyond their antibacterial potential, this class of compounds is also recognized for possessing antifungal [9], anticancer [10], antioxidant [7,11] and analgesic [12] activities, highlighting their broad pharmacological value. Aromatic azomethines also show tyrosinase inhibition activity [13].

The enduring scientific interest in the azomethines is driven by their structural adaptability, which allows for the strategic design of derivatives with tailored functionalities for specific technological and biomedical needs. The incorporation of long-chain substituents into azomethine frameworks presents a particularly promising research direction, as it enables precise modulation of their physicochemical characteristics, such as solubility, lipophilicity and etc., influencing practical efficacy. Azomethines with long alkyl chains and diethylamine substituent were synthesized [14] and biological activity measurements shown high efficacy against Gram positive and Gram negative bacterial strains and fungi. Adding 3d-metal complexes, the biocidal activity was increased remarkably, which was attributed to increased lipophilicity due to complexation with azomethines and enhanced penetration of metal ions through the lipid membrane, resulting in improved interaction with ferments [14].

The simplest way to obtain azomethines is reaction between aldehyde and amine [15]. Through the varying structures of both reagents a lot of combinations are possible. Such variability is important to obtain structure – properties correlations, which with relatively simple synthetic procedures for a lot of azomethines makes them attractive for robotic systems and autonomous (self-driving) labs [16].

Including another pharmacophore group into azomethine structure is also good way to obtain biologically active compounds. Thus, introduction triazole fragment gives substances with antifungal activity [17]. Azomethines with thiazole ring show anti-inflammatory and antioxidant activities [18]. A novel strategy for one-pot solvothermal synthesis were developed [19] and used to obtain phenylpyrazole Shiff bases, which works well as insecticides. Interestingly that this activity is attributed to the blocking of ionic channels due calcium chloride binding to C=N bond.

Nowadays a lot of new chemical substances are synthesized and biological activity measurements for all of them are hardly possible. So initial “filtration” with the real testing of the best revealed candidates seems more realistic scenario. Widely used method for biological activity predictions is docking, which is relatively fast for one molecule and one “target” (ferment molecule, DNA, RNA and etc.). However, in a living organism there are a lot of biomolecules for possible interactions and in combination with the necessity to predict activity for many molecules such investigations became very expensive in terms of computational time. Alternative way for predictions is quantitative structure-activity relationships (QSAR) modelling [20], which became powerful tool for high-throughput screening with the development of machine learning (ML) and artificial intelligence (AI).

Lipophilicity is very important property in drug discovery and design [21–23] and it is also necessary for good prediction of molecule bioactivity by machine learning. Usually lipophilicity is quantified as octanol-water partition coefficient (log*P*) and can be measured directly through the concentrations of substance in two phases by the shake-flask [24], slow-stirring [25] and generator column techniques [26]. Another possibility to determine lipophilicity is undirect methods, for example high-performance liquid chromatography [27], when log*P* is determined through the retention time, but such method works well only with the presence of reference substance with the known value of log*P*.

Experimental determination of lipophilicity can be unapplicable or give unreliable results for the poorly soluble substances. Similar problem with the highly hydrophilic or highly lipophilic compounds. In such cases computational approaches (for example, quantum-chemical calculations) or machine learning methods [28] can be the way for lipophilicity determination. Quantum-chemical determination of log*P* value is based on calculation of the Gibbs energy change upon transfer between solvents [29].

 doi:10.20944/preprints202512.1855.v1

The main aim of the work is the search of compounds with antibacterial properties and simple synthetic pathways, especially in combination with properties modelling technics, to use, in perspective, such systems for the development of autonomous labs [16], when predictions of artificial intelligence are tested by experiments on robotic installations and feedback is received on the results. The synthesized azomethines showed antibacterial activity at the level of some commercial antiseptics. Lipophilicity of the synthesized and isomeric substances was predicted using three different approaches: quantum chemical calculations, machine learning and fragment-based description. Machine learning-based methods (GraphormerLogP) demonstrate acceptable accuracy, sensitivity to isomerism, and orders of magnitude higher throughput, making them an optimal tool for high-throughput screening. Quantum-chemical calculations can take into account any spatial arrangements, but much more computational time it is necessary for it.

2. Materials and Methods

Commercially available reagents and solvents were used for synthesis.

The ^{1}H and $^{13}C\{^{1}H\}$ NMR spectra were recorded on Bruker Avance III 400 MHz spectrometer. Fourier Transform infrared spectroscopy (FT-IR) were measured using a FT-IR Spectrometer Spectrum two PerkinElmer with UATR (Single Reflection Diamond). Elemental analysis was made using PerkinElmer® 2400 Series II CHNS/O Elemental Analyzer (2400 Series II).

The antifungal and antibacterial activity of the chemical compounds was studied using test cultures of opportunistic microflora. The following strains were used: *Staphylococcus aureus* (ATCC 29213), *Escherichia coli* (ATCC 25922), *Pseudomonas aeruginosa* (ATCC 27853), *Bacillus cereus*, and *Candida albicans* (ATCC 885-653). All compounds are extremely poorly soluble in water, so 1% solutions in ethanol were used in the study.

24-hour cultures of microorganisms were washed from meat-peptone agar slants with saline and standardized to a turbidity standard of 0.5 McFarland ($1.5 \cdot 10^8$ CFU/ml). The culture media were inoculated with a swab soaked in the standardized culture. Wells were then cut in the contaminated nutrient agar and added with the test drugs and comparison drugs, Miramistin, Chlorhexidine and Kodan. Sabouraud's medium for *Candida* yeasts and Mueller-Hinton medium for pathogenic and opportunistic microflora of humans and animals were used as nutrient media. The dishes were incubated at 35 °C for 24-48 hours, after which the growth inhibition zone size was assessed, measuring it to an accuracy of 0.1 mm.

To complement the experimental investigation, the lipophilicity parameter ($\log P$, the octanol-water distribution coefficient) of the synthesized and isomeric compounds was estimated using quantum-chemical calculations, which were made using Orca program (version 6) [30,31]. r^{2}SCAN-3c composite method [32] was chosen as good cost-benefit-ratio method for structural optimizations and energy calculations [33]. SMD model [34] were used for accounting solvent effects; octanol and water were taken as solvents, structures were optimized at both solvents. Initial structures for calculations were made using Avogadro program [35]. Chemcraft [36] was used for calculations results viewing and visualization. Gibbs free energies were taken from calculations and $\log P$ was calculated using the formula:

$$\log P = \frac{\Delta G_{\text{water}} - \Delta G_{\text{octanol}}}{2.3RT}, \quad (1)$$

where ΔG_{water} – Gibbs free energy in water, $\Delta G_{\text{octanol}}$ – Gibbs free energy in octanol, R – universal gas constant, T – temperature (298 K).

Additionally, the lipophilicity parameter was estimated using a graph-based deep learning approach. For this purpose, we employed the GraphormerLogP model described in a recent publication [37], which demonstrated superior predictive accuracy compared to traditional descriptor-based and machine-learning methods. The GraphormerLogP model is based on a fine-tuned GraphormerMapper encoder architecture [38] that directly processes molecular graphs derived from SMILES strings. The molecular structures of the synthesized compounds were

 doi:10.20944/preprints202512.1855.v1

converted from SMILES representations into molecular graphs using the Chython library [39]. These graphs were subsequently processed by the pre-trained GraphormerLogP model with the original weights.

As an additional computational approach, lipophilicity (log*P*) values for the investigated compounds were estimated using the Crippen atom contribution model [40], as implemented in the Chem.Crippen module of the RDKit library [41]. The molecular structures of the investigated compounds were standardized and converted from SMILES representations into RDKit molecule objects. The lipophilicity was then computed using the MolLogP function, which reproduces the Wildman-Crippen model coefficients without additional parameter optimization. Due to its computational efficiency and reproducibility, this approach serves as a reliable baseline reference for comparing quantum-chemical log*P* estimates with machine learning-based predictions such as those obtained from the GraphormerLogP model.

3. Results

3.1. Compounds Synthesis and Characterization

Azomethines were synthesized according to the previously reported procedure [42] by the reaction between aromatic aldehyde with long-chain amine. Reaction in shown in Scheme 1; synthetic details are given in ESI1.

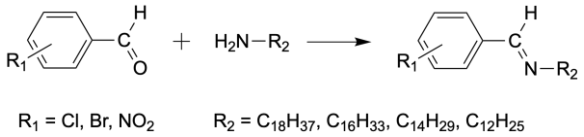

Scheme 1. Synthesis of azomethines.

The conformity of the obtained product with the expected structure was established on the basis of a set of data from elemental analysis, NMR and IR spectra (for details see ESI1). The yields are bigger than 90% (exact values can be found within synthetic details).

3.2. Rotation of Imine Fragment

Theoretically, the C=N double bond of imine fragment is in conjugation with phenyl ring and rotation around C(phenyl)-C(imine) bond may be difficult, so two ortho and two meta structures can be possible. That's why relaxed surface scans for the corresponding dihedral angle were made, results are shown in Figure 1 for the substances with C12 alkyl chain.

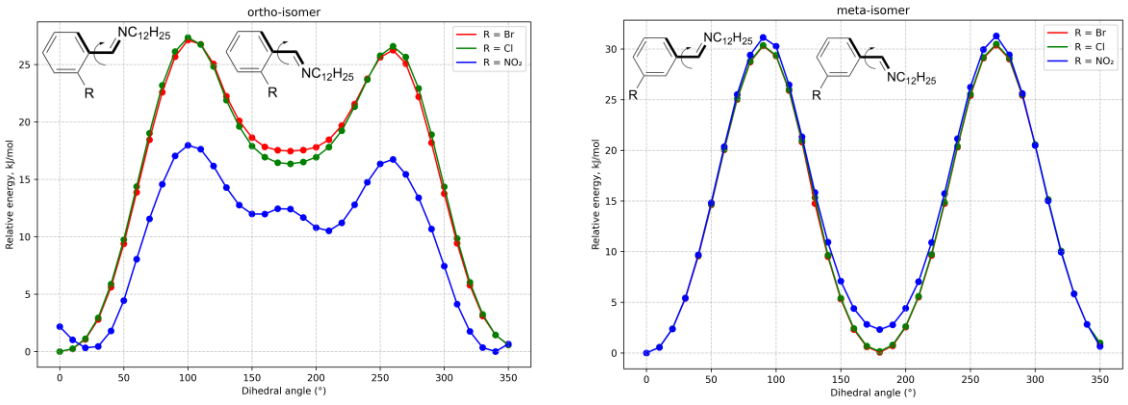

(**a**) (**b**)

Figure 1. Dependencies of relative energy from dihedral angle for ortho- (**a**) and meta- (**b**) isomers on the base of quantum-chemical calculations (r²SCAN-3c, vacuum). Bonds, forming fixed dihedral angle, are shown in bold on the inserted structures.

 doi:10.20944/preprints202512.1855.v1

As can be seen from the Figure 1, two minima are presented: in the first dihedral angle is 0° and nitrogen atom is in the opposite side of C(phenyl)-C(imine) bond relative to phenyl ring substituent; in the second angle is 180° and nitrogen is in the same side with heteroatomic group.

For the meta-isomer two minima have practically the same energies, whereas for ortho-isomer the difference is more than 15 kJ/mol for bromine and chlorine derivatives (for the nitro-substituted compound the difference is smaller – near 10 kJ/mol). Such situation can be explained by the steric hindrance between phenyl ring substituent and nitrogen atom of imine bond in the structures of ortho-isomers with the dihedral angle near 180°, when the atoms of mentioned fragments are very close to each other. In the meta-isomer substituent is in a more distant position from imine fragment, steric hindrance between those two groups is absent and energies of two minima are practically the same.

In the ortho-isomer of nitro-substituted compound minima are "twinned" – there are two small maxima at 0° and 180° with two minima at the both side of each. It should be mentioned that such "twinning" is absent in meta-isomer. Such situation is also the result of steric hindrance – at the "ideal" angles 0° and 180° nitro-group of ortho-isomer can't be located in the plane of phenyl ring, that's why conjugation between them is violated and energy is increased at 0° and 180° dihedral angles. Minima are shifted by some value (near 20-30°) to obtain optimal conjugation between the phenyl ring and both groups – nitro substituent and imine fragment. Structures, clarifying this situation, are given in Figure 2.

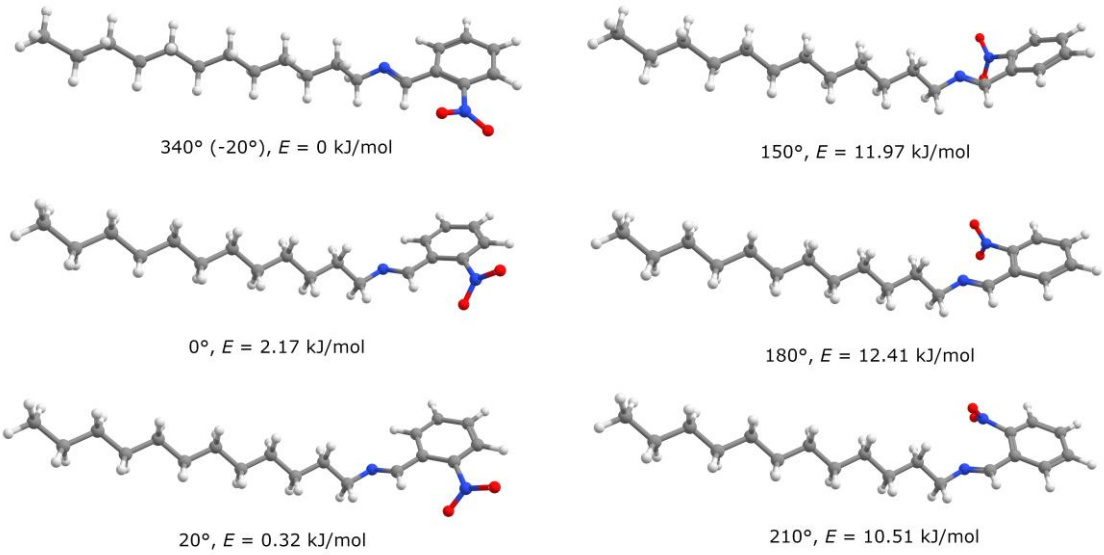

Figure 2. Structures of the nitro-substituted ortho-isomer with C12 alkyl chain for the different dihedral angles. Geometries, angle values and relative energies correspond to the energy profile in Figure 1a.

As can be seen from the Figure 1, energy barriers for the rotation are relatively low (the maximal value is near 30 kJ/mol), that's why the isomerization is highly possible at room temperature and structures for both local minima can be presented in solution. However, taking into account the energy difference between two minima for ortho-isomer, mole fraction of the structure with close arrangement of phenyl ring substituent and nitrogen atom of imine group is smaller than 1%. Similar equilibration between two structures of azomethine was observed for more complicated situation with cyclization [43].

 doi:10.20944/preprints202512.1855.v1

3.3. Antibacterial Activity

Antibacterial activity testing results are given in Table 1.

Table 1. Antibacterial activity of the investigated compounds in comparison with some antiseptics

N	Compound	The size of the growth inhibition zone, *d* (mm)				
		E. coli	*Bacillus cereus*	*P. aeruginosa*	*S. aureus*	*Candida albicans*
1	ortho-NO2C18	12±2	12±1	14±2	10±2	20±3
2	meta-NO2C18	15±3	14±3	22±3	11±1	0
3	para-NO2C18	10±1	10±1	11±3	10±1	17±3
4	meta-NO2C14	17±1	22±2	15±1	24±3	20±2
5	para-NO2C14	15±1	17±2	19±2	22±3	20±3
6	meta-NO2C12	17±2	22±3	15±4	24±5	20±2
7	para-NO2C12	15±3	17±4	19±2	22±4	20±3
8	para-BrC16	25±3	27±4	16±2	16±2	16±3
9	para-ClC16	10±1	14±2	0	0	11±1
10	“Kodan”	16±1	18±2	15±1	19±2	18±2
11	Miramistin	0	13±1	0	0	13±1
12	Chlorhexidine	0	13±1	0	0	13±1

As can be seen from the given data in Table 1, nine investigated compounds show the activity on the same level as antiseptic “Kodan” and works better for several test cultures than Miramistin and Chlorhexidine.

3.4. Lipophilicity Modelling

Lipophilicity modeling results obtained by three different methods (quantum chemical calculations (QC), GraphormerLogP model (GLP) and RDKit library (RDK)) are shown in Table 2 (optimized structures, xyz-matrices and energies for all isomers in Table 2 for both solvents (water and octanol) are given in ESI2).

To evaluate predictive accuracy, quantum-chemically computed logP values of azomethines were used as reference data. The GraphormerLogP deep learning model and the Wildman-Crippen atom contribution model were compared on this dataset. The GraphormerLogP model achieved higher overall accuracy (RMSE = 1.054 for all compounds, MAE = 0.943) than the RDKit predictions (RMSE = 1.407, MAE = 1.331).

As can be seen from the Table 2, logP modelling on the base of quantum-chemical calculations gives different results for all five structures (ortho, ortho’, meta, meta’ and para) as expected from different atom arrangements in 3d-space. GraphormerLogP approach doesn’t distinguish ortho/ortho’ and meta/meta’ pairs, which is not in controversary with relatively easy isomerization due to rotation (see section 3.2). Additionally, GLP method gives slightly different values for ortho-, meta- and para-isomers, the biggest difference is obtained for nitro derivative with C12 alkyl chain (0.27 log units, see Table 2). However, the relationships between values for ortho-, meta- and para-isomers in two methods (QC and GLP) are not the same for several substances in the Table 2. At the same time, RDKit method in such case is the worst of the used because doesn’t distinguish the position of substituent in phenyl ring (see Table 2).

Dependencies of modelled logP values from alkyl chain length are given in the Figure 3 for bromine and nitro derivatives (such dependency for chlorine derivatives is not shown, because it is very similar for bromine, see Table 2). The increasing of alkyl chain length leads to the increasing of

 doi:10.20944/preprints202512.1855.v1

logP value by QC method (adding two carbon atoms to the chain increase logP by the value near 1 log units).

Table 2. Predicted log*P* values (octanol – water) from quantum-chemical calculations (QC), GraphormerLogP model (GLP) and RDKit library (RDK).

isomer	alkyl chain											
	C12			C14			C16			C18		
	QC	GLP	RDK	QC	GLP	RDK	QC	GLP	RDK	QC	GLP	RDK
Bromine derivatives												
ortho	8.14	8.88	6.79	8.80	9.58	7.57	9.83	9.83	8.35	11.13	9.72	9.13
ortho'	7.93	8.88	6.79	8.95	9.58	7.57	10.06	9.83	8.35	10.95	9.72	9.13
meta	7.85	8.96	6.79	8.70	9.66	7.57	9.95	9.86	8.35	10.92	9.67	9.13
meta’	7.81	8.96	6.79	8.69	9.66	7.57	9.65	9.86	8.35	11.08	9.67	9.13
para	8.49	8.96	6.79	8.82	9.73	7.57	9.48	9.98	8.35	10.71	9.81	9.13
Chlorine derivatives												
ortho	7.95	8.86	6.68	8.78	9.69	7.46	9.86	10.00	8.24	11.02	9.82	9.02
ortho'	7.97	8.86	6.68	8.76	9.69	7.46	10.03	10.00	8.24	10.99	9.82	9.02
meta	7.74	8.80	6.68	8.67	9.68	7.46	9.71	9.97	8.24	10.77	9.77	9.02
meta’	7.67	8.80	6.68	8.79	9.68	7.46	9.77	9.97	8.24	10.68	9.77	9.02
para	7.63	8.88	6.68	8.75	9.74	7.46	10.69	10.02	8.24	11.93	9.84	9.02
Nitro derivatives												
ortho	7.06	8.28	5.93	7.93	9.25	6.71	9.20	9.83	7.50	10.12	9.87	8.28
ortho'	6.84	8.28	5.93	7.58	9.25	6.71	8.62	9.83	7.50	9.52	9.87	8.28
meta	6.42	8.01	5.93	7.23	9.01	6.71	8.44	9.70	7.50	9.46	9.90	8.28
meta’	6.55	8.01	5.93	7.44	9.01	6.71	8.61	9.70	7.50	9.55	9.90	8.28
para	6.68	8.09	5.93	7.47	9.05	6.71	8.55	9.76	7.50	8.80	9.98	8.28

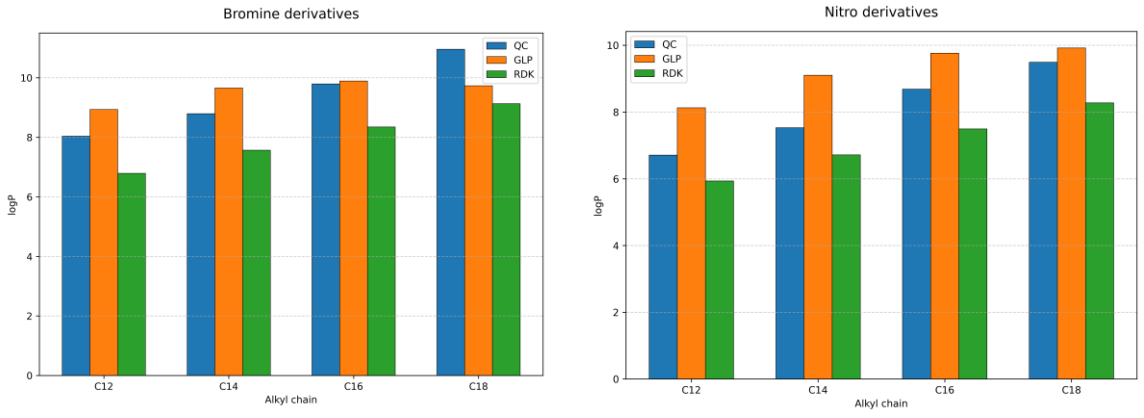

(**a**) (**b**)

Figure 3. Dependencies of modelled logP values from alkyl chain length for bromine (**a**) and nitro (**b**) derivatives. Mean values between different isomers were taken for QC and GLP methods.

For bromine derivatives (Figure 3a) with C12 and C14 alkyl chains, GraphormerLogP slightly overestimated lipophilicity, while for C16 compounds it showed the best agreement with QC values. Predictions for C18 compounds approached the upper limit of the model’s training range (logP =

 doi:10.20944/preprints202512.1855.v1

9.98), causing mild saturation and downward deviation relative to QC values. For nitro derivatives (Figure 3b) the best agreement between two methods (QC and GLP) is observed for C18 alkyl chain.

In contrast to this, the fragment-based model (RDK) consistently underestimates logP for all homologs, with MAE = 1.049, 1.111, 1.467, and 1.699 (mean values for bromine, chlorine and nitro derivatives together) for C12–C18, respectively.

It should be mentioned, that the three approaches differed markedly in computational efficiency. The quantum-chemical logP estimation required hundreds of hours for all 60 molecules, while GraphormerLogP completed predictions in several tens of seconds, and the Wildman–Crippen (RDKit) method finished in a few seconds, including environment initialization.

4. Discussion

Synthesized azomethines can be considered as perspective antibacterial agents due to their activity (see Table 1) and relatively simple synthesis (see experimental details in ESI1). However, very poor solubility in water and relatively low solubility in ethanol reduce these prospects. Despite this azomethines continue to be a good platform for the search for new pharmacological drugs, because changing substituents opens easy way to vary the properties of compounds.

Combination of three substituents (bromine, chlorine and nitro-group) at three positions (ortho-, meta- and para-) with four alkyl chains (C12, C14, C16 and C18) gives 36 possible compounds for the described platform with phenyl ring. Experimental synthesis and properties investigation of all substances “by hand” even at this relatively simple case looks impossible (if the developing field of the laboratory robotic systems and self-driving labs is not taken into account), so the initial “filtration” before real experiments is needed.

One of the important properties for the biological activity predictions is lipophilicity. Experimental measurements are very difficult for substances with very low solubility in water, so computational approaches come to the fore. In the present work three different methods were used: quantum-chemical calculations (QC), machine learning (GLP) and fragment-based approach (RDK).

On the base of quantum-chemical calculations logP can be determined for any structure, which corresponds to local (or global) minima, so the influence of conformational change, isomerization and tautomerization can be taken into account. However, this method is very time-consuming. Fragment based approach is very fast, but it is insensitive for the isomers with the same fragments (as in the investigated case with ortho-, meta- and para-isomers) and can give quite different results (underestimated for the studied azomethines). Machine-learning approach, such as used GraphormerLogP, is also fast, but is sensitive for isomers and can give better results than RDK.

Additionally, the initial 3d-structures are necessary for quantum-chemical calculations and generation of it is also the time-consuming step, whereas machine learning and fragment-based approaches need just text representation of molecule (for example, SMILES), generation of which can be easily automated for the similar compounds.

Thus, while quantum-chemical methods remain the reference standard for precision, deep learning and fragment-based approaches provide several orders of magnitude faster alternatives suitable for large-scale screening. Overall, GraphormerLogP predictions can be considered reliable within the explored lipophilicity range, offering a meaningful balance between accuracy and computational efficiency, with quantitative agreement to the quantum-chemical estimates.

5. Conclusions

Synthesized azometines represent promising antibacterial agents due to their pronounced activity and relatively simple synthesis. However, their potential is limited by their extremely low aqueous solubility. Despite this, this class of compounds remains a convenient platform for discovering new pharmacological substances, as varying substituents allows for targeted modification of the molecule's properties. Due to the need for preliminary virtual screening to select target structures from a multitude of possible derivatives, assessing lipophilicity (logP), which is

 doi:10.20944/preprints202512.1855.v1

difficult to measure experimentally, is crucial. Three computational approaches are compared: quantum chemical calculation (QC), machine learning (GLP), and fragment-based description (RDK). Despite the benchmark QC accuracy, which requires significant computational resources and three-dimensional structures, machine learning-based methods (GraphormerLogP) demonstrate acceptable accuracy, sensitivity to isomerism, and orders of magnitude higher throughput, making them an optimal tool for high-throughput screening.

Supplementary Materials: The following supporting information can be downloaded at the website of this paper posted on Preprints.org, Figures S1-1 – S1-13: NMR spectra; Figures S1-14 – S1-25: IR spectra; Figures S2-1 – S2-120: optimized structures of all compounds in water and octanol; Tables S2-1 – S2-120: cartesian coordinates for optimized structures; Tables S2-121 – S2-126: Gibbs free energies for optimized structures.

Author Contributions: Conceptualization, N.Yu.S. and Kh.R.Kh.; methodology, I.V.G. and T.R.G.; software, V.A.G. and T.R.G.; formal analysis, N.Yu.S., Kh.R.Kh., I.V.G. and T.R.G.; investigation, Kh.R.Kh., M.P.Sh. and V.A.G.; resources, N.Yu.S., I.V.G. and T.R.G.; data curation, Kh.R.Kh., M.P.Sh. and V.A.G.; writing—original draft preparation, N.Yu.S. and Kh.R.Kh.; writing—review and editing, N.Yu.S., Kh.R.Kh., V.A.G. and T.R.G.; visualization, N.Yu.S. and Kh.R.Kh.; supervision, N.Yu.S., I.V.G. and T.R.G.; project administration, N.Yu.S. and T.R.G.; funding acquisition, N.Yu.S. All authors have read and agreed to the published version of the manuscript.

Funding: The work was funded by financial support from the government assignment for FRC Kazan Scientific Center of RAS.

Data Availability Statement: The synthesis details, experimental spectra, optimized structures and calculated Gibbs energies are included in the supplementary materials.

Acknowledgments: The authors express sincere appreciation to Kazan Scientific Center of Russian Academy of Science for providing the research infrastructure and intellectual environment that enabled the quantum-chemical calculations and machine learning.

Conflicts of Interest: The authors declare no conflicts of interest. The funders had no role in the design of the study; in the collection, analyses, or interpretation of data; in the writing of the manuscript; or in the decision to publish the results.

Abbreviations

The following abbreviations are used in this manuscript:

AI	artificial intelligence
CFU	colony forming units
GLP	GraphormerLogP model
FT-IR	fourier transform infrared spectroscopy
MAE	mean absolute error
ML	machine learning
RDK	RDKit library
RMSE	root mean squared error
SMD	solvation model based on density
SMILES	simplified molecular input line entry system
QC	quantum chemistry
QSAR	quantitative structure-activity relationships

References

1. Hameed, A.; al-Rashida, M.; Uroos, M.; Abid Ali, S.; Khan, K.M. Schiff Bases in Medicinal Chemistry: A Patent Review (2010-2015). *Expert Opin. Ther. Pat.* **2017**, *27*, 63–79, doi:10.1080/13543776.2017.1252752.
2. Kajal, A.; Bala, S.; Kamboj, S.; Sharma, N.; Saini, V. Schiff Bases: A Versatile Pharmacophore. *J. Catal.* **2013**, *2013*, 893512, doi:10.1155/2013/893512.

 doi:10.20944/preprints202512.1855.v1

3. Ceramella, J.; Iacopetta, D.; Catalano, A.; Cirillo, F.; Lappano, R.; Sinicropi, M.S. A Review on the Antimicrobial Activity of Schiff Bases: Data Collection and Recent Studies. *Antibiotics* **2022**, *11*, 191, doi:10.3390/antibiotics11020191.
4. Pencheva, I.; Peikova, L.; Tsvetkova, D. Pharmacological Applications of Azomethine Derivatives in the Therapy of Different Diseases. *Pharmacia* **2025**, *72*, 1–17, doi:10.3897/pharmacia.72.e159352.
5. Shekhar, S.; Khan, A.M.; Sharma, S.; Sharma, B.; Sarkar, A. Schiff Base Metallodrugs in Antimicrobial and Anticancer Chemotherapy Applications: A Comprehensive Review. *Emergent Mater.* **2022**, *5*, 279–293, doi:10.1007/s42247-021-00234-1.
6. Pervaiz, M.; Sadiq, A.; Sadiq, S.; Saeed, Z.; Imran, M.; Younas, U.; Majid Bukhari, S.; Rashad Mahmood Khan, R.; Rashid, A.; Adnan, A. Design and Synthesis of Schiff Base Homobimetallic-Complexes as Promising Antimicrobial Agents. *Inorg. Chem. Commun.* **2022**, *137*, 109206, doi:10.1016/j.inoche.2022.109206.
7. Shanty, A.A.; Philip, J.E.; Sneha, E.J.; Prathapachandra Kurup, M.R.; Balachandran, S.; Mohanan, P.V. Synthesis, Characterization and Biological Studies of Schiff Bases Derived from Heterocyclic Moiety. *Bioorganic Chem.* **2017**, *70*, 67–73, doi:10.1016/j.bioorg.2016.11.009.
8. Iqbal, A.; Siddiqui, H.L.; Ashraf, C.M.; Ahmad, M.; Weaver, G.W. Synthesis, Characterization and AntibacterialActivity of Azomethine Derivatives Derived from 2-Formylphenoxyacetic Acid. *Molecules* **2007**, *12*, 245–254, doi:10.3390/12020245.
9. Patil, S.A.; Prabhakara, C.T.; Halasangi, B.M.; Toragalmath, S.S.; Badami, P.S. DNA Cleavage, Antibacterial, Antifungal and Anthelmintic Studies of Co(II), Ni(II) and Cu(II) Complexes of Coumarin Schiff Bases: Synthesis and Spectral Approach. *Spectrochim. Acta. A. Mol. Biomol. Spectrosc.* **2015**, *137*, 641–651, doi:10.1016/j.saa.2014.08.028.
10. Sztanke, K.; Maziarka, A.; Osinka, A.; Sztanke, M. An Insight into Synthetic Schiff Bases Revealing Antiproliferative Activities in Vitro. *Bioorg. Med. Chem.* **2013**, *21*, 3648–3666, doi:10.1016/j.bmc.2013.04.037.
11. Zubair, M.; Sirajuddin, M.; Ullah, K.; Haider, A.; Perveen, F.; Hussain, I.; Ali, S.; Tahir, M.N. Synthesis, Structural Peculiarities, Theoretical Study and Biological Evaluation of Newly Designed O-Vanillin Based Azomethines. *J. Mol. Struct.* **2020**, *1205*, 127574, doi:10.1016/j.molstruc.2019.127574.
12. Chinnasamy, R.; Sundararajan, R.; Govindaraj, S. Synthesis, Characterization, and Analgesic Activity of Novel Schiff Base of Isatin Derivatives. *J. Adv. Pharm. Technol. Res.* **2010**, *1*, 342, doi:10.4103/0110-5558.72428.
13. Bae, S.J.; Ha, Y.M.; Park, Y.J.; Park, J.Y.; Song, Y.M.; Ha, T.K.; Chun, P.; Moon, H.R.; Chung, H.Y. Design, Synthesis, and Evaluation of (E)-N-Substituted Benzylidene–Aniline Derivatives as Tyrosinase Inhibitors. *Eur. J. Med. Chem.* **2012**, *57*, 383–390, doi:10.1016/j.ejmech.2012.09.026.
14. Negm, N.A.; Zaki, M.F.; Salem, M.A.I. Cationic Schiff Base Amphiphiles and Their Metal Complexes: Surface and Biocidal Activities against Bacteria and Fungi. *Colloids Surf. B Biointerfaces* **2010**, *77*, 96–103, doi:10.1016/j.colsurfb.2010.01.012.
15. Sprung, M.A. A Summary of the Reactions of Aldehydes with Amines. *Chem. Rev.* **1940**, *26*, 297–338, doi:10.1021/cr60085a001.
16. Sanchez-Lengeling, B.; Aspuru-Guzik, A. Inverse Molecular Design Using Machine Learning: Generative Models for Matter Engineering. *Science* **2018**, *361*, 360–365, doi:10.1126/science.aat2663.
17. Sun, X.; Bai, Y.; Liu, Y.; Chen, B.; Jia, Y.; Zeng, Z. Synthesis and Biological Activity of 4,5-Dihydro-1,2,4-Triazole-5-Thione Schiff Base. *Chin. J. Chem.* **2009**, *27*, 1397–1400, doi:10.1002/cjoc.200990234.
18. Geronikaki, A.V., Paola; Incerti, Matteo; Hadjipavlou-Litina, Dimitra Thiazolyl and Isothiazolyl Azomethine Derivatives with Anti-Inflammatory and Antioxidant Activities. *Arzneimittelforschung* **2004**, *54*, 530–537, doi:10.1055/s-0031-1297008.
19. Chen, L.; Wu, Z.; Du, Y.; Huang, Y.; Jin, S. Solvothermal Synthesis of Novel Phenylpyrazole Schiff Base Fluorescent Insecticides Fused Extended Conjugate Units for Enhancing Bioactivities, Photophysical and Electrochemical Properties. *J. Mol. Struct.* **2019**, *1196*, 555–566, doi:10.1016/j.molstruc.2019.06.093.
20. Muratov, E.N.; Bajorath, J.; Sheridan, R.P.; Tetko, I.V.; Filimonov, D.; Poroikov, V.; Oprea, T.I.; Baskin, I.I.; Varnek, A.; Roitberg, A.; et al. QSAR without Borders. *Chem. Soc. Rev.* **2020**, *49*, 3525–3564, doi:10.1039/D0CS00098A.
21. Waring, M.J. Lipophilicity in Drug Discovery. *Expert Opin. Drug Discov.* **2010**, *5*, 235–248, doi:10.1517/17460441003605098.

 doi:10.20944/preprints202512.1855.v1

22. Arnott, J.A.; Planey, S.L. The Influence of Lipophilicity in Drug Discovery and Design. *Expert Opin. Drug Discov.* **2012**, *7*, 863–875, doi:10.1517/17460441.2012.714363.
23. Tsopelas, F.; Giaginis, C.; Tsantili-Kakoulidou, A. Lipophilicity and Biomimetic Properties to Support Drug Discovery. *Expert Opin. Drug Discov.* **2017**, *12*, 885–896, doi:10.1080/17460441.2017.1344210.
24. Ma, Y.; Chen, X.; Javeria, H.; Du, Z. High-Throughput Screening of LogD by Using a Sample Pooling Approach Based on the Traditional Shake Flask Method. *J. Chromatogr. B* **2023**, *1227*, 123804, doi:10.1016/j.jchromb.2023.123804.
25. De Bruijn, J.; Busser, F.; Seinen, W.; Hermens, J. Determination of Octanol/Water Partition Coefficients for Hydrophobic Organic Chemicals with the "Slow-Stirring" Method. *Environ. Toxicol. Chem.* **1989**, *8*, 499–512, doi:10.1002/etc.5620080607.
26. Woodburn, K.B.; Doucette, W.J.; Andren, A.W. Generator Column Determination of Octanol/Water Partition Coefficients for Selected Polychlorinated Biphenyl Congeners. *Environ. Sci. Technol.* **1984**, *18*, 457–459, doi:10.1021/es00124a012.
27. Terada, H. Determination of Log Poct by High-Performance Liquid Chromatography, and Its Application in the Study of Quantitative Structure-Activity Relationships. *Quant. Struct.-Act. Relatsh.* **1986**, *5*, 81–88, doi:10.1002/qsar.19860050302.
28. Win, Z.-M.; Cheong, A.M.Y.; Hopkins, W.S. Using Machine Learning To Predict Partition Coefficient (Log P) and Distribution Coefficient (Log D) with Molecular Descriptors and Liquid Chromatography Retention Time. *J. Chem. Inf. Model.* **2023**, *63*, 1906–1913, doi:10.1021/acs.jcim.2c01373.
29. Roy, D.; Patel, C. Revisiting the Use of Quantum Chemical Calculations in LogPoctanol-Water Prediction. *Molecules* **2023**, *28*, 801, doi:10.3390/molecules28020801.
30. Neese, F. The ORCA Program System. *WIREs Comput. Mol. Sci.* **2012**, *2*, 73–78, doi:https://doi.org/10.1002/wcms.81.
31. Neese, F. Software Update: The ORCA Program System—Version 6.0. *Wiley Interdiscip. Rev. Comput. Mol. Sci.* **2025**, *15*, e70019, doi:10.1002/wcms.70019.
32. Grimme, S.; Hansen, A.; Ehlert, S.; Mewes, J.-M. r2SCAN-3c: A "Swiss Army Knife" Composite Electronic-Structure Method. *J. Chem. Phys.* **2021**, *154*, 064103, doi:10.1063/5.0040021.
33. Bursch, M.; Mewes, J.-M.; Hansen, A.; Grimme, S. Best-Practice DFT Protocols for Basic Molecular Computational Chemistry**. *Angew. Chem. Int. Ed.* **2022**, *61*, e202205735, doi:10.1002/anie.202205735.
34. Marenich, A.V.; Cramer, C.J.; Truhlar, D.G. Universal Solvation Model Based on Solute Electron Density and on a Continuum Model of the Solvent Defined by the Bulk Dielectric Constant and Atomic Surface Tensions. *J. Phys. Chem. B* **2009**, *113*, 6378–6396, doi:10.1021/jp810292n.
35. Hanwell, M.D.; Curtis, D.E.; Lonie, D.C.; Vandermeersch, T.; Zurek, E.; Hutchison, G.R. Avogadro: An Advanced Semantic Chemical Editor, Visualization, and Analysis Platform. *J. Cheminformatics* **2012**, *4*, 17, doi:10.1186/1758-2946-4-17.
36. Chemcraft - Graphical Software for Visualization of Quantum Chemistry Computations. Version 1.8, Build 780. Https://Www.Chemcraftprog.Com.
37. Grigorev, V.; Serov, N.; Gimadiev, T.; Poyezzhayeva, A.; Sidorov, P. Graph-based transformer to predict the octanol-water partition coefficient. J. Chemoinformatics. In press.
38. Nugmanov, R.; Dyubankova, N.; Gedich, A.; Wegner, J.K. Bidirectional Graphormer for Reactivity Understanding: Neural Network Trained to Reaction Atom-to-Atom Mapping Task. *J. Chem. Inf. Model.* **2022**, *62*, 3307–3315, doi:10.1021/acs.jcim.2c00344.
39. Fallani, A.; Nugmanov, R.; Arjona-Medina, J.; Wegner, J.K.; Tkatchenko, A.; Chernichenko, K. Pretraining Graph Transformers with Atom-in-a-Molecule Quantum Properties for Improved ADMET Modeling. *J. Cheminformatics* **2025**, *17*, 25, doi:10.1186/s13321-025-00970-0.
40. Wildman, S.A.; Crippen, G.M. Prediction of Physicochemical Parameters by Atomic Contributions. *J. Chem. Inf. Comput. Sci.* **1999**, *39*, 868–873, doi:10.1021/ci990307l.
41. RDKit Available online: http://www.rdkit.org/ (accessed on 14 October 2025).
42. Galkina, I.V.; Kiyamova, E.R.; Gaynullin, A.Z.; Bakhtiyarov, D.I.; Shulaeva, M.P.; Pozdeev, O.K.; Egorova, S.N.; Ivshin, K.A.; Kataeva, O.N.; Bakhtiyarova, Y.V.; et al. Synthesis and Structure of Novel

 doi:10.20944/preprints202512.1855.v1

Phosphorylated Azomethines. *Phosphorus Sulfur Silicon Relat. Elem.* **2016**, *191*, 1679–1681, doi:10.1080/10426507.2016.1227822.

43. Salih, K.S.M. Solvent Influence on Absorption Spectra and Tautomeric Equilibria of Symmetric Azomethine-Functionalized Derivatives: Structural Elucidation and Computational Studies. *ChemistryOpen* **2022**, *11*, e202100237, doi:10.1002/open.202100237.